

# **Integrating Phenotypic and Chemoproteomic Approaches to Identify Covalent Targets of Dietary Electrophiles in Platelets**

*Ivy A. Guan<sup>1,2</sup>, Joanna S.T. Liu<sup>2,3</sup>, Renata C. Sawyer<sup>1,2</sup>, Xiang Li<sup>4,5</sup>, Wanting Jiao<sup>6</sup>, Yannasittha Jiramongkol<sup>1,8</sup>, Mark D. White<sup>1</sup>, Lejla Hagimola<sup>3</sup>, Freda H. Passam<sup>3</sup>, Denise P. Tran<sup>7</sup>, Xiaoming Liu<sup>3</sup>, Simone M. Schoenwaelder<sup>2,3</sup>, Shaun P. Jackson<sup>2,8</sup>, Richard J. Payne<sup>1,9</sup>, Xuyu Liu<sup>\*1,2</sup>*

<sup>1</sup>School of Chemistry, Faculty of Science, The University of Sydney, Sydney, New South Wales 2006, Australia

<sup>2</sup>The Heart Research Institute, The University of Sydney, Newtown, New South Wales 2042, Australia

<sup>3</sup>School of Medical Sciences, Faculty of Medicine and Health, The University of Sydney, Sydney, New South Wales 2006, Australia

<sup>4</sup>Department of Medicine, Washington University in St. Louis, St. Louis, MO 63110, United States

<sup>5</sup>McDonnell Genome Institute, Washington University in St. Louis, St. Louis, MO 63108, United States

<sup>6</sup>Ferrier Research Institute, Victoria University of Wellington, Wellington 6140, New Zealand; Maurice Wilkins Centre for Molecular Biodiscovery, Auckland 1142, New Zealand.

<sup>7</sup>Sydney Mass Spectrometry, The University of Sydney, Camperdown, New South Wales 2006, Australia

<sup>8</sup>Charles Perkins Centre, The University of Sydney, Sydney, New South Wales 2006, Australia

<sup>9</sup>Australian Research Council Centre of Excellence for Innovations in Peptide and Protein Science, The University of Sydney, Sydney, New South Wales 2006, Australia

**KEYWORDS:** Electrophilic natural products; Platelets; Covalent inhibition; Activity-based protein profiling; Thrombosis; Antiplatelets; Stroke; Phytochemicals

**ABSTRACT:** A large variety of dietary phytochemicals have been shown to improve thrombosis and stroke outcomes in preclinical studies. Many of these compounds feature electrophilic functionalities that potentially undergo covalent addition to the sulfhydryl side chain of cysteine residues within proteins. However, the impact of such covalent modifications on platelet activity and function remains unclear. In this study, we evaluated phenotypes associated with irreversible protein engagement of twenty-three electrophilic phytochemicals. This revealed a novel antiplatelet selectivity profile of the isothiocyanate-containing natural product sulforaphane (SFN), whereby the response of platelets to adenosine diphosphate (ADP) and a thromboxane A<sub>2</sub> receptor agonist was impaired without affecting thrombin and collagen-related peptide (CRP) activation. SFN also substantially reduces the formation of platelet thrombi on surfaces coated with collagen under arterial flow conditions. Activity-based protein profiling identified protein disulfide isomerase A6 (PDIA6) as a rapid kinetic responder of SFN. Mechanistic profiling studies revealed how SFN fine-tunes the enzymatic activity and substrate specificity of PDIA6. In an electrolytic injury model of thrombosis, SFN enhanced the thrombolytic activity of recombinant tissue plasminogen activator (rtPA) without increasing blood loss. Our results serve as a catalyst for further investigations into the preventive and therapeutic mechanisms of dietary antiplatelets, with a view to develop more effective and safer adjunctive treatments to improve the clot-busting power of rtPA – currently the sole approved therapeutic for stroke recanalization that has significant limitations.

**INTRODUCTION:** Platelets are crucial cellular components of the blood that orchestrate hemostasis, preventing blood loss by forming stable clots in response to vascular injury. However, they also play a major role in thrombosis, eliciting an exaggerated thrombotic response when exposed to pathological conditions including atherosclerotic plaque rupture (1), disturbed fluid flow (1), and elevated blood velocity (2). Pathological thrombosis may obstruct blood flow in veins, arteries, or smaller vessels, inhibiting the delivery of essential nutrients like glucose and oxygen to critical organs. Platelet-mediated thrombosis underlies the development of numerous cardiovascular diseases, including ischemic stroke (3) and myocardial infarction (heart attack) (4). Collectively, these diseases account for the leading cause of death and disability globally, making them a massive burden on healthcare systems and carers (5, 6).

Over the past three decades, significant advancements have been made in identifying the fundamental mechanisms of platelet function and activation (1, 7). These discoveries have advanced antiplatelet therapeutic development. However, currently approved antithrombotic strategies do not effectively discriminate between hemostasis and thrombosis, and inhibit critical platelet functions relevant for hemostasis, for example, the inhibition of the major platelet integrin  $\alpha_{IIb}\beta_3$  (GPIIb-IIIa) (8), which can cause life-threatening bleeding complications. Therefore, a better understanding of the unique signaling processes that differentiate platelet-mediated thrombosis and hemostasis could facilitate the development of targeted antithrombotic therapies that do not increase bleeding risk. Antithrombotics, including antiplatelet agents, have been shown to improve reperfusion therapy in the acute coronary syndromes, and are now incorporated into the standard-of-care regimen as adjuncts for thrombolytic therapy (9, 10); the efficiency of vessel recanalization/reperfusion is closely linked to improve patient outcomes (11). However, all current antiplatelet agents are contraindicated for adjunctive therapies for thrombolysis in stroke patients, due to the high risk of symptomatic brain hemorrhage, which is the most feared complication of thrombolytic therapy (8, 12).

A large variety of dietary phytochemicals have been identified as potential thromboprophylaxis that could enhance the outcomes of stroke treatment and management (13-16). These compounds also demonstrate favorable tolerability and safety profiles in individuals with thrombotic or bleeding disorders (15, 17-19). Many dietary phytochemicals possessing  $\alpha,\beta$ -unsaturated carbonyl (20, 21), isothiocyanate (22) and other electrophilic functionalities, have been associated with covalent modulation of proteins influencing transcription factors (23) and other gene-regulatory machineries (24). An archetypal response occurs through covalent inhibition of the E3 ligase Keap1, which in turn liberates the Nrf2 transcription factor to upregulate expression of antioxidant and detoxification enzymes (23, 25). Despite these advances, our understanding of their influence on platelet reactivity is still limited, as the conventional model of transcriptional regulation plays a limited role in regulating platelet function, due to the absence of a functional genome in platelets.

In this study, our objective was to characterize the antiplatelet phenotypes associated with the covalent modification of proteins by dietary phytochemicals (**Figure 1**). As part of this work, we sought to identify the most impacted targets, and also highlight the potential long-term consequences related to the dietary consumption of these compounds. Given the limited capacity of platelets to resynthesize proteins (26, 27), covalent protein modifications are anticipated to have a more profound impact on platelet (patho)physiology compared to other human cell types. In this report, we introduce an integrated phenotypic and Activity-Based Protein Profiling (ABPP) approach to examine the prevalence of covalent modifications induced by plant-derived natural products with  $\alpha,\beta$ -unsaturated, isothiocyanate and a mixture of electrophilic moieties.

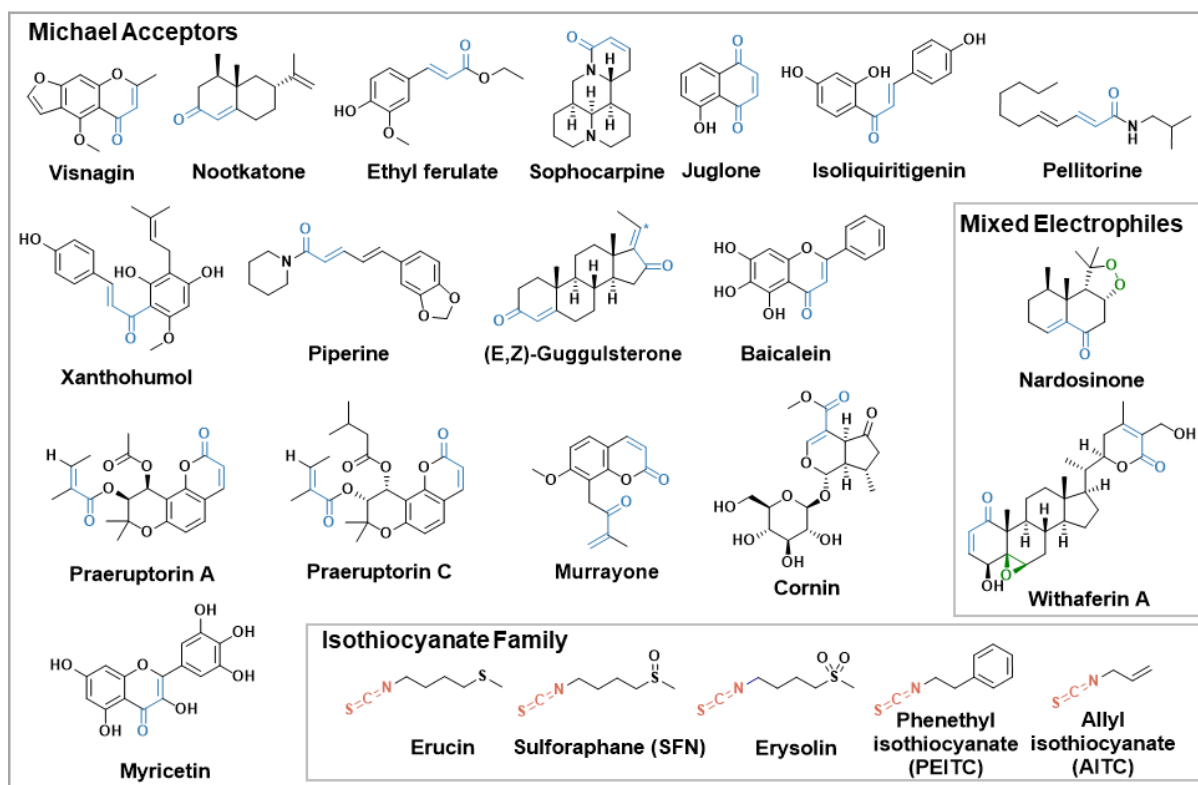


**Figure 1.** Chemical structures of selected natural products with electrophilic functional groups highlighted in blue (Michael acceptors), green (epoxide and peroxide) and red (isothiocyanate).

## RESULTS AND DISCUSSION:

### A Streamlined Preparation Protocol for Interrogating Irreversible Platelet Inhibition

Numerous natural products interact with protein targets through a blend of reversible and irreversible binding modes (28). In particular, several archetypal phytochemicals found in diets and in herbal medicines, once thought to promote health benefits via reversible binding to proteins, have now been found to operate via covalent modes of inhibition that result in long-lasting changes of protein activity and function (29-35). We envisaged that the biological influence of covalent engagement could be effectively assessed via jump-dilution and washout experiments, two methods frequently employed to examine the impact of irreversible inhibitors on cellular activity (36, 37). We began with integrating a washout procedure into our platelet preparation protocol (**Figure S2**). This involved pelleting compound- or vehicle-treated

platelets and subjecting them to a wash protocol with a standard platelet wash buffer (PWB, see **Supporting Information Section 2.1**). Subsequently, the platelets were resuspended in physiological Tyrode's buffer for aggregation assays. Although encouraging antiplatelet effects of several natural products were initially uncovered, a marked decrease in platelet activity, including in the control sample, was observed one-hour post-washout. This phenomenon may be attributed to the increased handling of platelets, which may inadvertently activate the cells and decrease the overall viability of the platelet population. As such, we devised an alternative approach by incorporating the jump-dilution method into our platelet preparation protocol (see **Supporting Information Section 2.1**). Briefly, freshly isolated platelets were incubated with the PWB containing 20  $\mu\text{M}$  of the natural product for 120 minutes at 37 °C to facilitate potential covalent engagement. Subsequently, the platelets were pelleted and subjected to a 200-fold dilution in volume with Tyrode's buffer to achieve a final concentration of  $3 \times 10^8$  cells/mL. The functional activity of these platelets was examined in a medium-throughput manner by employing light transmission aggregometry.

### **Distinct Antiplatelet Activity Profiles Associated with Irreversible Modulation by Dietary Electrophiles**

Here we present a summary of the activity profiles for twenty-three dietary natural products (21, 22, 38, 39) (**Figure 1**), depicted as a heatmap to illustrate their effects against four commonly encountered agonists, ADP, thrombin, collagen related peptide (CRP) and the thromboxane A2 analog U46619 (**Figure 2A**). The natural product library of choice includes eighteen  $\alpha,\beta$ -unsaturated carbonyl compounds and five isothiocyanate compounds, all of which were selected based on their reported antithrombotic roles as constituents of heart-healthy diets, nutraceutical supplements, and herbal medicines (21, 22, 38, 39). To account for donor variability, residual platelet activities were normalized to the vehicle control from the same donor. Interestingly, we found that a substantial portion (65%) of these compounds, featuring Michael acceptor functionalities, did not demonstrate inhibitory effects on platelets

under our jump-dilution conditions. This observation notably differs from earlier reports (40, 41), where some natural products exhibited antiplatelet activities when introduced concurrently with an agonist. This process, referred to as the 'direct addition' method (**Figure 2B**), implies that their antiplatelet effects are likely to be reversible.

The active samples identified through the 'jump-dilution' protocol can be categorized into two main clusters according to their selectivity profiles: Cluster 1 includes juglone, while Cluster 2 consists of the isothiocyanate family, withaferin A and xanthohumol. Juglone exhibited a wide range of inhibitory activities, effectively eliminating platelet responsiveness in all aggregometry settings. Our finding aligns with the antiplatelet activity of juglone documented by Wu and colleagues (38) and further substantiates the notion that juglone irreversibly modifies the platelet proteome, as expected for the highly reactive nature of the quinone motif found in the molecule. In contrast to Cluster 1, molecules in Cluster 2 displayed selectivity towards certain thrombogenic biochemical stimuli, while preserving platelet reactivity to thrombin (0.05 – 0.1 U/mL). This observation is potentially important, as currently approved antiplatelet agents cannot distinguish signaling initiated by thrombin, the central protease in blood coagulation, from other agonistic pathways (42). In particular, these agents' capacity to impair the activation of the platelet glycoprotein (GP) Ib complex during thrombin-induced platelet aggregation has become an important parameter to evaluate their bleeding risks (43-46).

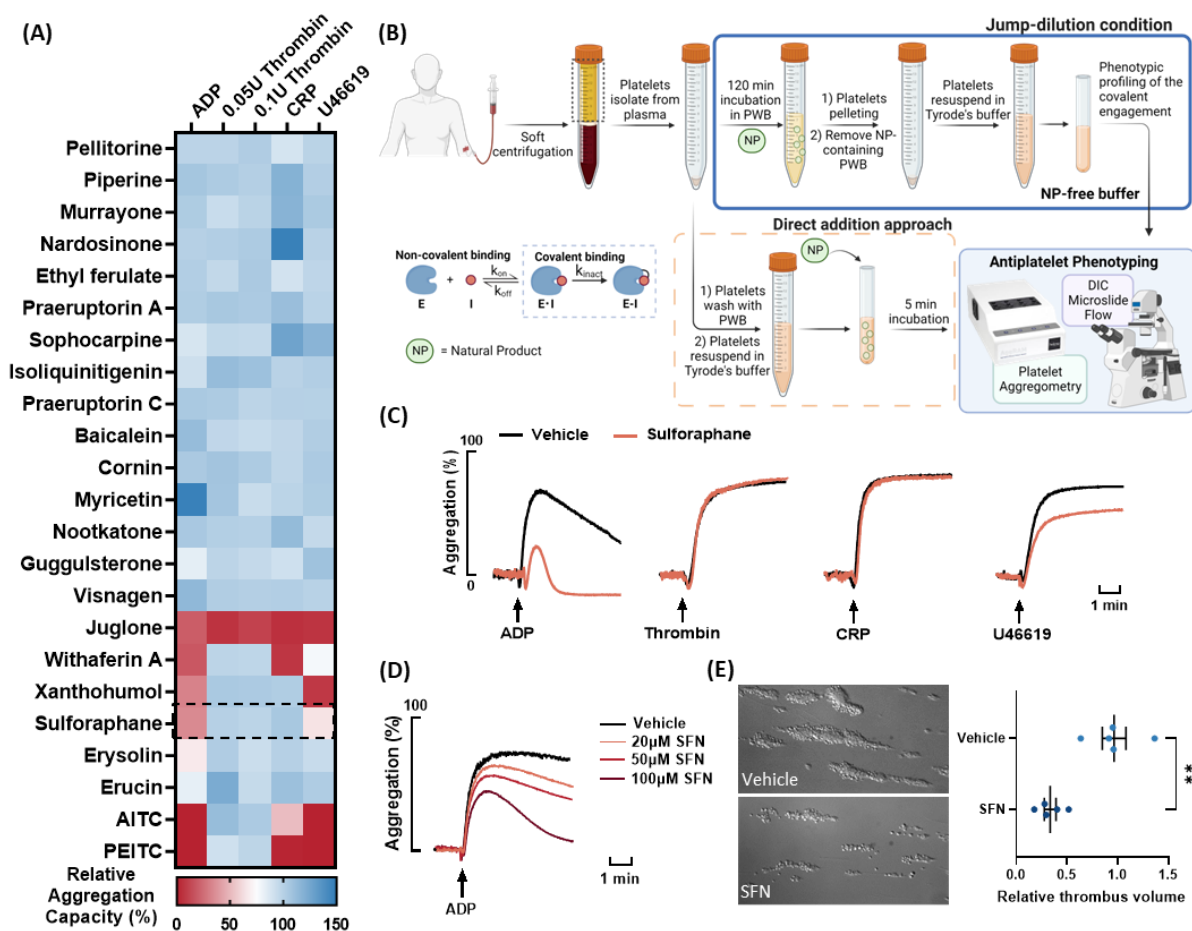


**Figure 2. Antiplatelet phenotypic screening of electrophilic phytochemicals.** (A) Heatmap depicts the effects of natural products (20  $\mu$ M) on platelet activities in response to ADP (2-5  $\mu$ M), thrombin (0.05-0.1 U/mL), collagen-related peptide (CRP, 0.5 mg/mL), and U46619 (0.2–0.5  $\mu$ M) induced aggregation, following a jump-dilution preparation procedure. Relative aggregation capacity (%) was calculated according to **Figure S3**. (B) Schematic illustration of the platelet washing and natural product incubation workflow: the ‘jump-dilution’ approach and the conventional ‘direct addition’ approach employed to examine the antiplatelet activities. (C) Representative light-transmission platelet aggregometry profiles: the aggregation activity profiles of SFN and vehicle-treated platelets (under jump-dilution conditions) in response to ADP (5  $\mu$ M), thrombin (0.05 U/mL), CRP (0.5 mg/mL) and U46619 (0.5  $\mu$ M) are shown. (D) Representative light-transmission platelet aggregometry profiles: the ADP aggregation profiles (5  $\mu$ M) of platelets treated with 20–100  $\mu$ M SFN through the conventional ‘direct addition’ method. (E) Thrombi formation in



80  $\mu\text{M}$  SFN- or vehicle-treated whole blood at a shear rate of  $1800\text{ s}^{-1}$  for 2 minutes were visualized under a differential interference contrast (DIC) microscope (63x, water objective). SFN inhibits platelet thrombus formation under arterial flow conditions ( $1800\text{ s}^{-1}$ ). Relative thrombus volume was measured by labeling the platelets with DiOC6 for 1 hour followed by fixation with 2% paraformaldehyde, confocal volumetric imaging (Nikon Eclipse Ti, 40x water objective), and 3-dimensional quantification with NIS-Elements AR.5.21.03 (**Figure S8**). Volumetric data was shown as mean  $\pm$  SEM and unpaired t-test was used to compare the treatment.

### **Sulforaphane Manifests a Novel Agonist Selectivity Profile in Platelet Inhibition**

Among the five isothiocyanate natural products, withaferin A and xanthohumol in Cluster 2, the selectivity exhibited by SFN, a natural product derived from broccoli sprouts, caught our attention: SFN exhibited a unique preference for inhibiting ADP, while its minimal or absent effect on U46619-induced aggregation varied depending on the donor. Notably, platelet aggregation induced by thrombin and CRP remained unaffected across a wide spectrum of agonist concentrations (**Figure 2A**). This ADP selective profile was consistently observed with 12 healthy human donors, spanning both sexes and an age range of 18 to 60 years. Assaying platelets prepared through our 'washout' protocol also confirmed the selectivity [**Figure S4(B)**]. Our subsequent structure-activity relationship (SAR) study revealed the importance of SFN's sulfoxide center for biological activity. Reducing or oxidizing the sulfoxide moiety to form erucin or erysolin resulted in a decrease in the inhibitory activity (**Figure 2A**). Further alterations to the aliphatic chain of SFN may also jeopardize its agonist selectivity, as evidenced by the antiplatelet activity profiles of allyl isothiocyanate (AITC) and phenethyl isothiocyanate (PEITC).

## SFN Suppresses Shear-Induced Thrombus Formation

To further investigate the functional influence of SFN under more physiologically relevant conditions, we evaluated the dynamics of platelet adhesion on type I collagen under arterial flow conditions, using a microslide perfusion system (47). Anticoagulated whole blood was obtained from healthy donors and perfused through the collagen-coated microslide at high arterial shear rates ( $1800 \text{ s}^{-1}$ ). As illustrated in **Figure 2E**, during a 2-minute perfusion of whole blood, platelets adhered to the collagen-coated surfaces and formed large aggregates in vehicle-treated controls. However, a significant reduction in platelet adhesion and thrombus size was observed when whole blood was pre-treated with  $80 \mu\text{M}$  SFN for 1 hour. The platelets within the thrombi were subsequently labeled with DiOC6, and the total thrombus volume across the entire microslide was quantified, revealing a 64% decrease in thrombus size compared to the vehicle-treated controls (**Figure S8**).

## Leveraging an Activity-Based Probe of SFN to Map the Covalently Modulated Protein Targets

Given that SFN is known to covalently modify the side chain functionalities of cysteine and lysine residues within proteins, it is widely recognized as a polypharmacological agent that influences multiple targets simultaneously (22). A few protein targets modulated by SFN have been discovered and characterized, providing a preliminary understanding of its chemopreventive and anti-inflammatory benefits (48, 49). However, their roles in the modulation of platelet function and prevention of thrombotic disorders have yet to be confirmed (50, 51).

In light of SFN's multi-target modulation, ABPP presents itself as a promising and robust technique for providing a wholistic understanding of the covalently modified proteome (48, 49). It has also become the gold-standard approach for profiling both on- and off-target effects of covalent drugs (52-56). Furthermore, recent technological advancements in ABPP enable quantification of target occupancy and selectivity and measurement of labeling kinetics. This

advancement sets the stage for identifying the most sensitive druggable sites based on locale, temporal factors, and disease specificity, which is of great significance for electrophilic drug discovery (57-63). Cole and colleagues previously documented the development and utilization of a cell-permeable alkyne-tagged ABPP probe to mimic SFN (48). In this probe, the key reaction functionalities such as isothiocyanate and sulfoxide groups were replaced with sulfoxythiocarbamate and a ketone, respectively. In light of our SAR studies, which highlight the critical roles of sulfoxide and isothiocyanate of SFN for agonist selectivity, we aimed to develop SFNp – a SFN-based probe that retains the essential functionalities with an alkyne reporter to facilitate target enrichment and mapping studies. A nitrile analog (NCOp) of the SFNp was also prepared and served as a negative control (**Figure 3B**). The antiplatelet activities of SFNp and NCOp were first examined under standard jump-dilution conditions; SFNp phenocopied SFN in light-transmission aggregometry and microslide flow assays, whereas NCOp did not display significant antiplatelet activities in these experiments (**Figure S5&S8**). To validate the intracellular covalent engagement, live platelets were preincubated with SFNp (20  $\mu$ M), NCOp (20  $\mu$ M) or an equivalent volume of vehicle (DMSO) in PWB for varying durations followed by centrifugation and removal of the probe-containing buffer. The resulting platelet pellets were immediately lysed and subjected to Cu(I)-catalyzed azide-alkyne cycloaddition (CuAAC) coupling with Cy5 azide for in-gel fluorescence analysis, or with biotin azide for streptavidin-mediated target enrichment. Through in-gel fluorescence analysis, we confirmed the establishment of covalent bonds between SFNp and protein targets through reactions at the isothiocyanate group, as compared to the lack of Cy5 fluorescence signals detected in the proteome treated with NCOp (**Figure 3C**). On the other hand, biotin-enriched SFNp-modified proteins were first resolved on SDS-PAGE gels, followed by gel excision, in-gel digestion and LC-MS/MS analysis to identify the target proteins. The protein signals obtained were normalized against background signals, which were enriched through an identical workflow, except that DMSO (vehicle) or NCOp was employed instead of SFNp (**Supplementary proteomic data file 1**).

We recruited platelet samples from three healthy donors for our target mapping studies. Following a 2-hour treatment with SFNp, we identified a total of 298 significant hits as compared to the NCOp control (**Figure 3D**); significant hits are defined as those showing a four-fold enrichment relative to the control. These hits encompass a wide variety of proteins with diverse biological functions, such as catalytic activity, transport functions, and carrier responsibilities (**Figure 3E**). Notably, 63% of these hits have not been previously investigated for drug discovery, underscoring the effectiveness of this ABPP approach in identifying novel targets (**Figure 3E**). Among the 298 hits, 14 proteins were identified as common hits shared by all three donors, some of which are already known to regulate platelet activity (**Supplementary proteomic data file 1**). For instance, transforming growth factor beta-1 proprotein (TFGB1) is involved in the wound healing and scarring pathway and is released from  $\alpha$ -granules upon platelet activation (64). However, for the majority of these common hits, their functional roles in platelet-induced thrombosis are still unclear.

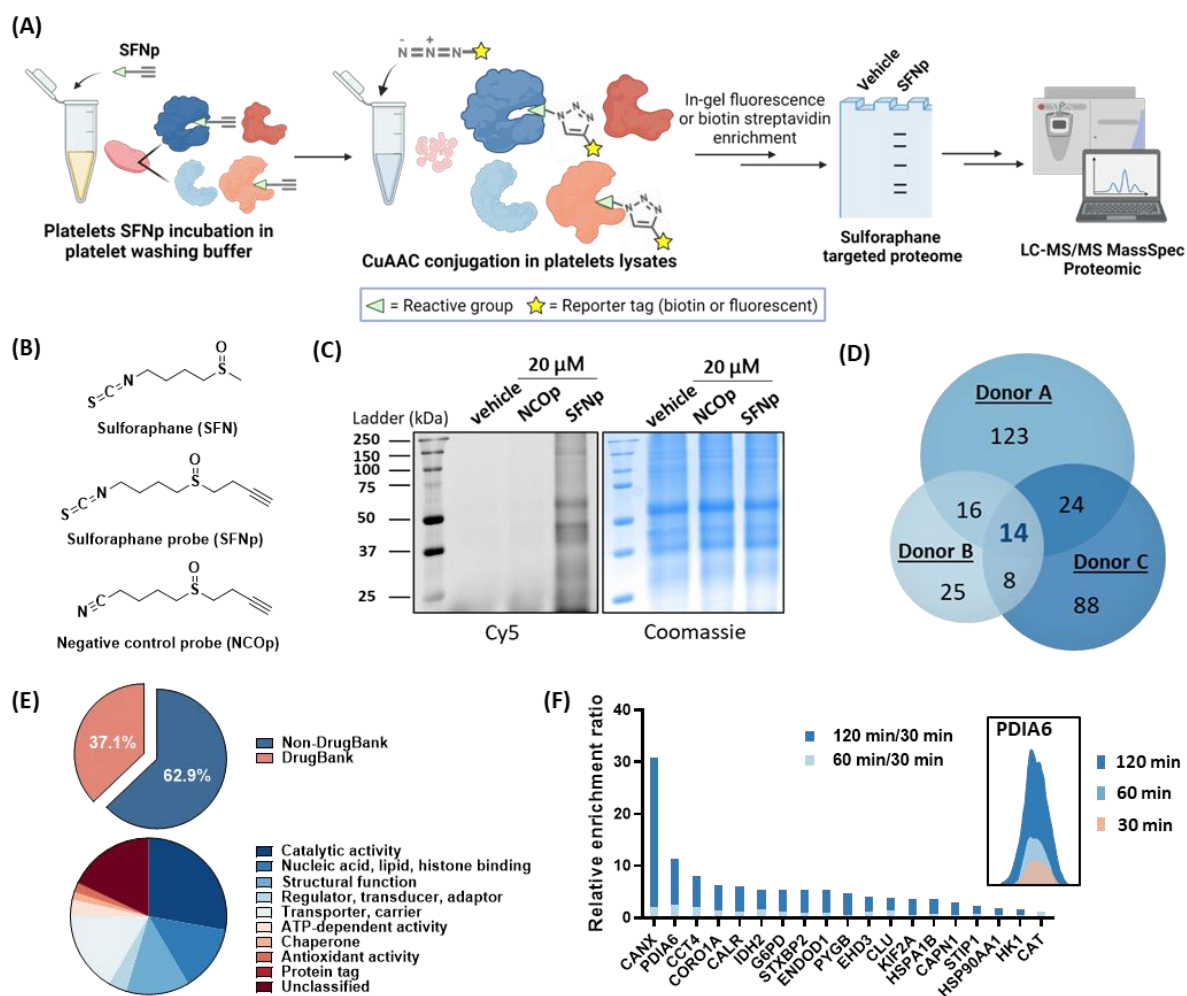


**Figure 3. Proteomic mapping of platelet targets covalently modulated by SFN activity-based probe. (A)** Schematic illustration showing the treatment of live platelets with SFNp and downstream target analysis. **(B)** Chemical structures of sulforaphane (SFN), SFN activity-based probe (SFNp) and the negative control probe (NCOp). **(C)** In-gel fluorescence analysis of proteins revealed from SFNp, NCOp or vehicle (DMSO) pre-treated platelets. The structural analog NCOp (20  $\mu$ M) without an isothiocyanate functionality was incapable of labeling the proteome as compared to SFNp and vehicle. Coomassie stained proteins were used as the loading control. **(D)** Venn diagrams depict protein targets enriched by SFNp using a biotin-streptavidin affinity purification workflow, followed by in-gel tryptic digestion for LC-MS/MS analysis. Platelets pre-exposed to NCOp (20  $\mu$ M) or an equivalent volume of vehicle (DMSO) served as a negative control, with the resulting proteomic samples prepared through the same process. Peptide intensities from the SFNp treatment samples, as determined by mass

spectrometry, have been normalized against control samples. Significant hits are defined as those showing a four-fold enrichment relative to the controls. This Venn diagram specifically outlines these hits relative to the NCOp sample. For significant hits normalized against the vehicle sample, refer to **Figure S10. (E)** Functional classification of all identified SFNp-enriched protein targets (found in  $\geq 1$  donors) based on DrugBank protein database released on 04/01/2023. **(F)** Protein disulfide isomerase A6 (PDIA6) was a common significant hit identified in all donor samples and exhibited a preponderance in covalent labeling by SFNp compared to the other common hits (found in 2-3 donors).

### **Kinetic Analysis Reveals PDIA6 as a Dominant Responder to SFN in Live Platelets**

We anticipated that by comparing the target labeling kinetics of SFN in live platelets, we would be able to identify the genuine target(s) responsible for the time-dependent inhibition of platelet aggregation induced by ADP [**See Figure S4(B) middle graph**]. As such, a new kinetic study was performed, in which a donor's platelets were incubated with 20  $\mu\text{M}$  SFNp for 30, 60, and 120 minutes. Subsequently, extensive washing was carried out to remove unbound SFNp, followed by cell lysis and CuAAC conjugation to biotin for enrichment and LC-MS/MS analysis (**Figure 3F**). The MS1 signals derived from the 30-minute labeling sample were employed as a control group for mass spectrometry signal normalization, as the influence on platelet activity at this specific time point was found to be minor. From our analysis, we identified nineteen proteins exhibiting a kinetic response to SFNp covalent modification (**Figure 3F**). Of these, calnexin and protein disulfide isomerase A6 (PDIA6) stood out as major kinetic responders to SFN treatment, showing a more than 10-fold increase in covalent engagement after a 2-hour incubation with SFNp in live platelets, compared to the control. Calnexin, an endoplasmic reticulum (ER)-resident chaperone, has a crucial role in folding N-linked glycoproteins within the ER and is known to regulate the biogenesis of integrin GPIIb-IIIa in megakaryocytes (65). However, given that platelets inherit the folded GPIIb-IIIa from megakaryocytes and possess a limited ability to produce new integrin proteins (26, 27), the impact of SFN-modified calnexin

on platelet adhesion and aggregation via integrin over a short period, such as within the period of 2-hour incubation, is expected to be minimal. Therefore, attention was shifted to the second prominent kinetic responder PDIA6, which was consistently identified across all tested donor samples (n=4) via this ABPP approach.

PDIA6, a member of the 20-enzyme thiol isomerase family, primarily facilitates protein folding by catalyzing the formation and cleavage of disulfide bonds in the ER, while also acting as a negative regulator of ER stress pathways (66). Recent studies have underscored the importance of PDIA6, alongside PDIA1 and PDIA3, in folding and activating integrins and receptors on the surface of platelets, endothelial cells and lymphocytes (67). In particular, PDIA6 has been found to facilitate thrombus formation in a mouse model of laser-induced thrombosis (68). PDIA6, as well as other thiol isomerase enzymes, are characterized by the presence of thioredoxin-like domains (69, 70), and in PDIA6, three such domains are present: **a**, **a'**, and **b**. Both the **a** and **a'** domains are catalytically active and contain a CGHC motif in the active site. In contrast, the **b** domain lacks this motif but possesses two cysteine residues with functions that have not yet been determined (71).

### **C291 and C297 of PDIA6 are Isoform-Specific Cysteines Modified by SFN**

To determine whether PDIA6 was responsible at least in part for the action of SFN on platelet function that we observed, we first assessed the influence of SFN on PDIA6 structure, function and activity. We expressed the full-length 48 kDa His6-PDIA6 recombinantly in accordance with the protocol published previously (67). Its disulfide-reducing activity was assessed using the standard insulin aggregation assay (72) before proceeding with any assay and mass spectrometry studies.

We began with determining the in vitro labeling kinetics. Reduced PDIA6 (20  $\mu$ M) was incubated with 1.25 equiv. SFNp (25  $\mu$ M) followed by a 20-fold dilution in denaturing buffer (2% SDS, 50 mM HEPES, 150 mM NaCl, pH 7.4) and assayed with CuAAC conjugation to Cy5

azide. **Figure 4A** displays a time-dependent increase in the Cy5 signal, with a half-life of covalent labeling at 29 minutes.

To identify the covalent modification site(s), PACMA31, a covalent pan-PDI inhibitor, was used as a benchmark for targeting the catalytic cysteines within the **a** domain of PDIA6 (73); it was our initial hypothesis that SFN would target a similar site. Reduced PDIA6 (20  $\mu$ M) was labeled with 1.1 or 10 equivalents of SFN followed by treatment with 1 mM N-propargylmaleimide (MA) to cap any unmodified cysteines. To our surprise, the **b**-domain cysteines in PDIA6 emerged as the primary modification sites for SFN (**Figure 4B&C**). When using 1.1 equivalents, either one of the **b**-domain cysteine residues (C291 or C297) was labeled, together with Lys85 without any other off-site labeling identified (**Figure S11**). Despite being unable to identify the CGHC motif in the **a'** domain, SFN labeling of catalytic cysteine residues within the **a** domain was not observed at either concentration, as determined by comparative analysis with the control sample involving the addition of MA alone or PACMA31 followed by MA capping (**Figure S11&S12**). To the best of our knowledge, SFN is the first PDI modulator that covalently modifies non-catalytic cysteines within the **b** domain of PDIA6. Notably, among the seven highly homologous human PDIs, PDIA6 stands out as the sole member containing two cysteines at this specific position (**Figure 4D**). This discovery raises the possibility of PDI isoform-selective modulation through a naturally-occurring covalent modification strategy.



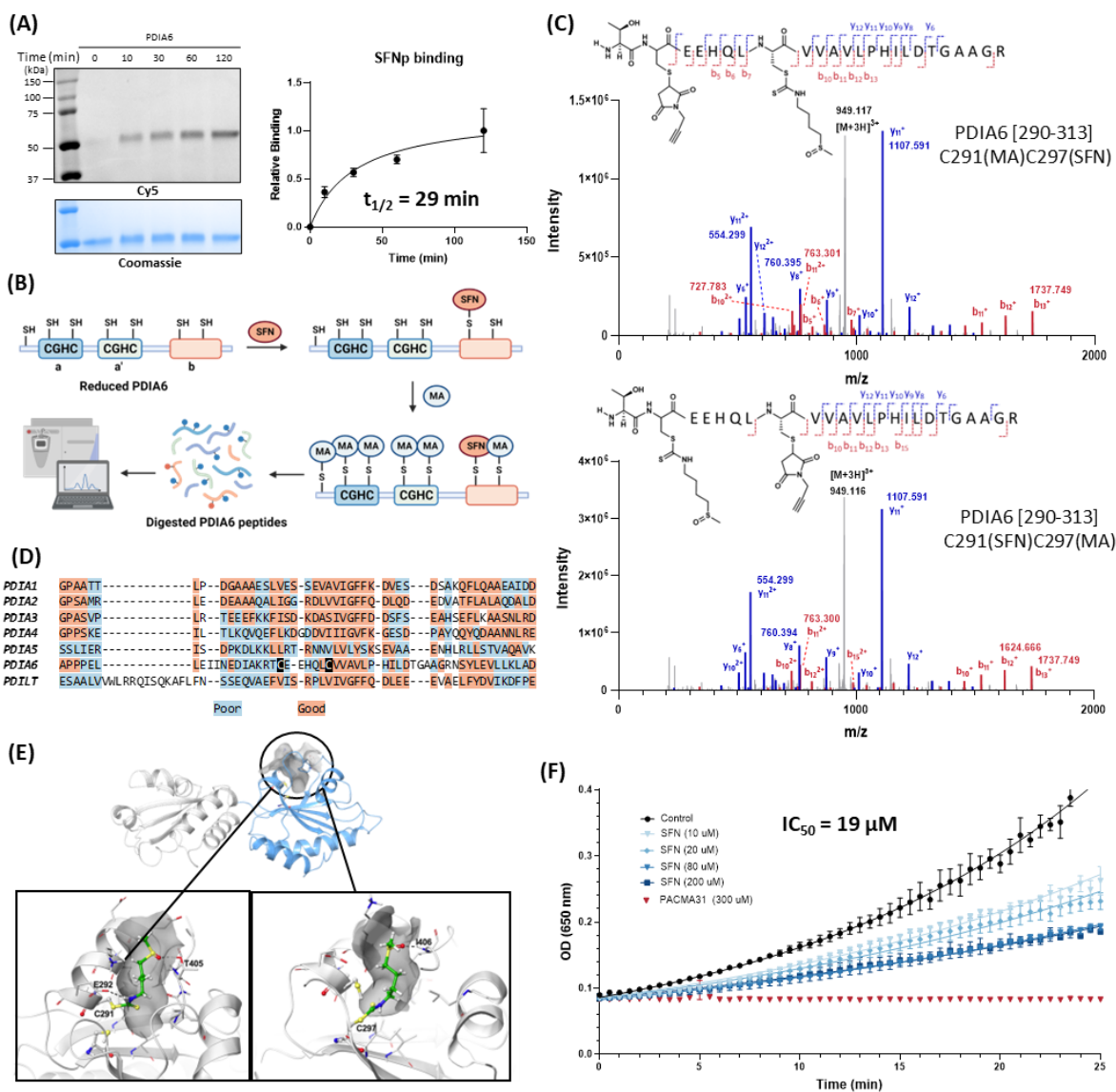


**Figure 4. PDIA6 is an isoform-selective and kinetically-privileged sensor of SFN.**

**(A)** Time-responsive covalent association analysis of PDIA6 labeling by SFNp. Recombinantly expressed PDIA6 was first reduced by DTT (10 mM) for 30 minutes before undergoing gel filtration on a Zeba Spin desalting column (7 K molecular weight cut-off, 0.5 mL). The resulting PDIA6 (20  $\mu$ M) was treated with SFNp (25  $\mu$ M) in 50 mM HEPES/150 mM NaCl (pH 7.4) for varying time intervals (0, 10, 30, 60 and 120 minutes) at 37  $^{\circ}$ C prior to CuAAC conjugation to Cy5 in denaturing conditions. **(B)** Schematic illustration of the workflow for PDIA6 modification site identification by LC-MS/MS. Reduced PDIA6 (20  $\mu$ M) was treated with SFN (22  $\mu$ M) in 50 mM HEPES/150mM NaCl (pH 7.4) for 1 hour before adding 1 mM N-propargylmaleimide (MA). The resulting mixture was subjected to standard trypsin

digestion and LC-MS/MS analysis. **(C)** Representative MS/MS spectra of PDIA6(290-313) peptide labeled by SFN and MA at C291 and C297. **(D)** Sequence alignment of the **b** domain of seven PDI isoforms. SFN-sensing sites (C291 and C297 residues) in PDIA6 are highlighted in black. **(E)** Molecular modeling of SFN into the potential binding pocket on the **b**-domain of PDIA6. Molecular dynamics simulation on the AlphaFold model of the **a'**-**b** domains of PDIA6 revealed potential binding pocket near the Cys291 and Cys297 (grey surface representation). Conformations of SFN (green carbon) covalently linked to either Cys291 (box on the left) or Cys297 (box on the right) were predicted through a series of molecular modeling studies, including rigid receptor ligand docking, induced fit docking and covalent docking calculations. Details of the computational methods are described in the **Supporting Information Section 4**. **(F)** Insulin turbidity assay demonstrated the comparative impact on PDIA6 activity via covalent modulation by SFN and PACMA31, respectively. Reduced PDIA6 (5  $\mu$ M) was treated with SFN or PACMA31 at varying concentrations (10, 20, 80, 200 or 300  $\mu$ M) at 37 °C for 1 hour before adding to 0.1 M  $K_2HPO_4$  (pH 7.0), 2 mM EDTA, 0.13 mM bovine insulin, and 0.33 mM dithiothreitol, yielding a final concentration of 100 nM PDIA6.

### **Molecular Dynamics Simulation Reveals the Unique Binding Mode of SFN**

Molecular modeling studies were subsequently performed to investigate how SFN may bind to the **b**-domain of PDIA6. A 400 ns molecular dynamics (MD) simulation on the AlphaFold model (74) of the **a'**-**b** domains of human PDIA6 revealed a potential binding pocket near the two cysteine residues of interest. Analysis of the protein surface using SiteMap (75, 76) identified a narrow binding pocket located between the helix consisting of residues 284-292 and the loop comprising residues 403-406 (**Figure 4E**). A series of ligand docking calculations using the software Glide (77-79), including rigid receptor ligand docking and induced fit docking (80-82), were conducted (**Supporting information Section 4**) to refine the binding pocket conformations and optimize interactions with SFN. The final conformations of SFN covalently bound to either Cys291 or Cys297 were obtained from covalent docking

calculations (**Figure S19**), which were predicted with favorable binding affinities [molecular mechanics with generalized Born and surface area (MM-GBSA) scoring] for the non-covalent interactions with the surrounding residues (-37.7 kcal/mol and -34.8 kcal/mol, respectively). In line with our SAR studies, the sulfoxide functionality was anticipated to improve site selectivity and binding affinity via polar interactions with the side chains of Glu292 and Thr405, as well as the backbone amide of Ile406 (**Figure 4E**).

### **Bioinformatic Analysis Reveals the Altered Interactome of PDIA6 upon SFN Covalent Labeling and Supports the Agonist Selectivity Profile of SFN**

Next, we characterized the impact of C291/C297 covalent modifications on disulfide isomerase activity. Reduced PDIA6 (5  $\mu$ M) was preincubated with varying concentrations of SFN (10, 20, 80, and 200  $\mu$ M) at 37 °C for one hour, with the intention of establishing the covalent engagement prior to enzymatic assessment. This was followed by a 50-fold dilution in the assay buffer containing 0.1 mM  $K_2HPO_4$  (pH 7.0), 2 mM EDTA, 0.13 mM bovine insulin, and 0.1 mM DTT. We observed that SFN exhibited the characteristics of a partial antagonist: even at very high concentrations (i.e., 200  $\mu$ M), only a 60% reduction in PDIA6 activity was observed (**Figure 4F**). This phenomenon may be attributed to the structural nuances induced by the covalent modification of the **b** domain cysteines, which could influence PDIA6's substrate preference without eliminating the catalytic activity towards disulfide substrates. We were therefore interested in studying the substrate scope of covalently modified PDIA6 by conducting an interactome co-precipitation experiment (**Figure 5A**). His6-PDIA6 protein with or without prior incubation with SFN, was utilized to enrich its interactome from platelet lysate on Ni-NTA agarose beads. Following this, the proteins were eluted from the beads and resolved on SDS-PAGE gels for in-gel trypsin digestion and LC-MS/MS analysis. This experiment was replicated on three donor samples (**Supporting information Section 3.7**). Our study uncovered clear evidence of a distinct interactome of PDIA6 as a result of covalent modulation by SFN (**Figure 5B and Supporting Information Section 3.8**).

LC-MS/MS in conjunction with Ingenuity Pathway Analysis (IPA) bioinformatic analysis reveals that the SFN-labeled PDIA6 displays an increased affinity to PI3K $\gamma$  with a lower affinity for PIK3IP1, a negative regulator of PI3Ks (**Supplementary proteomic data file 2**). The Gi-coupled ADP receptor P2Y<sub>12</sub> is known to facilitate PI3K $\gamma$  activation upon platelet stimulation, supporting platelet function by maintaining integrin  $\alpha$ IIb $\beta$ 3 activation (83). The PI3K $\gamma$  isoform has also been found to support platelet activation downstream of the ADP receptor P2Y<sub>12</sub> in a selective manner; the aggregation response to ADP, but not collagen and thrombin, is significantly reduced in platelets deficient in PI3K $\gamma$  *in vivo* (83-85). Based on this analysis, we hypothesize that SFN increases PDIA6's affinity to PI3K $\gamma$ , leading to selective modulation of ADP signaling, which in turn attenuates the response of platelets to ADP in our aggregometry setting. Our observation also aligns with previous studies where SFN was demonstrated to exhibit characteristics of PI3K inhibitors against platelets under flow conditions (50).

Our study further reveals that SFN enhances PDIA6's affinity toward multiple GDP/GTP exchange proteins (GEP), potentially influencing RhoA activity, a regulator of platelet contractility and thrombus stability (86, 87). Reduced RhoA signaling could impact thrombus stability and clot retraction, consistent with the observed decrease in stable platelet aggregate formation under arterial flow conditions (**Figure 2E**). Our findings align with previous studies that reveal the functional connections between various PDI isoforms and signaling players in RhoGTPase pathways through co-immunoprecipitation studies and conserved gene microsynteny approaches (88, 89). Moreover, SFN-labeled PDIA6 also exhibits an elevated binding affinity for STIM, implying a potential influence on Ca<sup>2+</sup> influx, an essential factor governing platelet shape changes, adhesion, and coagulation (90).

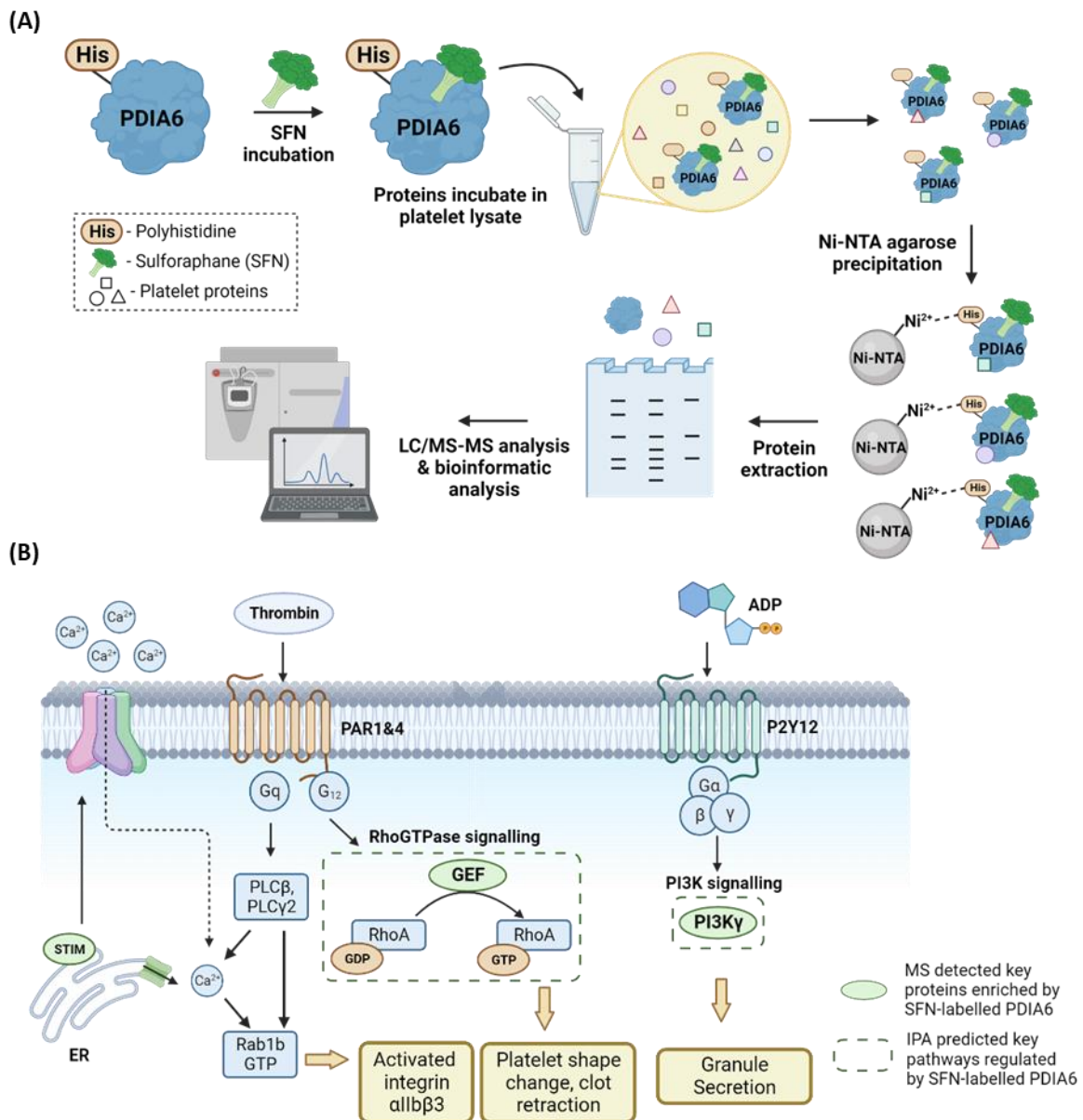


**Figure 5. Integrated bioinformatic analysis reveals the pathways modulated by SFN-modified PDIA6. (A)** Schematic illustration of the workflow of PDIA6 interactome enrichment. His6-PDIA6 (0.84  $\mu$ M) was incubated with 20  $\mu$ M SFN followed by addition to platelet lysates in a standard, non-denaturalizing lysis buffer. Correlated proteins were enriched on Ni-NTA agarose beads followed by extraction and resolution on an SDS-PAGE gel. In-gel tryptic digestion followed by LC-MS/MS analysis were conducted to reveal the binding profiles. **(B)** The reconstruction of protein networks was based on results from IPA as well as

literature searching. The relevant signal transduction pathways and selected proteins enriched in these pathways are annotated.

### **SFNp Enhances Thrombolysis Efficacy without Causing Excess Bleeding In Vivo**

Based on our *in vitro* data and bioinformatic analysis of PDIA6 interactome, we hypothesized that platelets pre-exposed to SFNp would form a less stable clot, rendering it more susceptible to thrombolytic therapy. Therefore, we next focused on investigating the therapeutic synergy between SFNp and thrombolysis with recombinant tissue plasminogen activator (rtPA), the only approved therapy for stroke, utilizing an *in vivo* electrolytic model of thrombosis (**Figure 6A**). Briefly, C57Bl/6 mice were anaesthetized and subjected to an electrolytic injury (8 mA, 3 minutes) (91), forming an occlusive thrombus in the left carotid artery. To assess the effectiveness of SFNp to promote the thrombolytic activity of rtPA, we examined recanalization outcomes compared to mice treated with rtPA alone. Recanalization was evaluated by assessing blood flow (mL/min) using a doppler flow probe and defined and categorized as specified: no recanalization – no return of flow following injury and occlusion, transient recanalization – momentary return of flow after clot formation, followed by reocclusion (no flow), and stable recanalization – flow returns to the vessel at similar levels before the injury and is sustained. Initial studies in untreated mice revealed that recanalization rates achieved with rtPA alone (1 mg/kg bolus, 9 mg/kg infusion) were relatively low, with only 17% of mice demonstrating a transient recanalization event (n=2/12) while the majority of mice (83%) demonstrated sustained occlusion (n=10/12), with no mice demonstrating stable recanalization (0%). Our initial experiments confirmed that without prior exposure to SFNp, co-administration of SFNp (50 mg/kg bolus) with rtPA (1 mg/kg bolus, 9 mg/kg infusion) did not significantly improve carotid recanalization [83% no recanalization (n=5/6), 17% transient recanalization (n=1/6), and 0% stable recanalization] (**Figure 6B**). In stark contrast, pre-incubation with SFNp for 1 hour prior to electrolytic injury resulted in a significant improvement in recanalization efficacy, with 12.5% no recanalization (n=1/8), 62.5% transient recanalization

(n=5/8), and 25% stable recanalization (n=2/8). Notably, our study also demonstrated that the aforementioned dose (50 mg/kg) of SFNp did not cause excessive blood loss, as assessed through a standard 3-mm tail lop assay (92), measuring the amount of hemoglobin lost over the observation period (**Figure 6C**). Interestingly, this was despite an equivalent or additional number of re-bleeding events compared to saline-treated mice (**Figure 6C**), which may relate to the stability of the blood clot. This data affirms the *in vivo* safety of the SFN mimic SFNp alongside its thrombolytic efficacy in a murine model of thrombolysis.

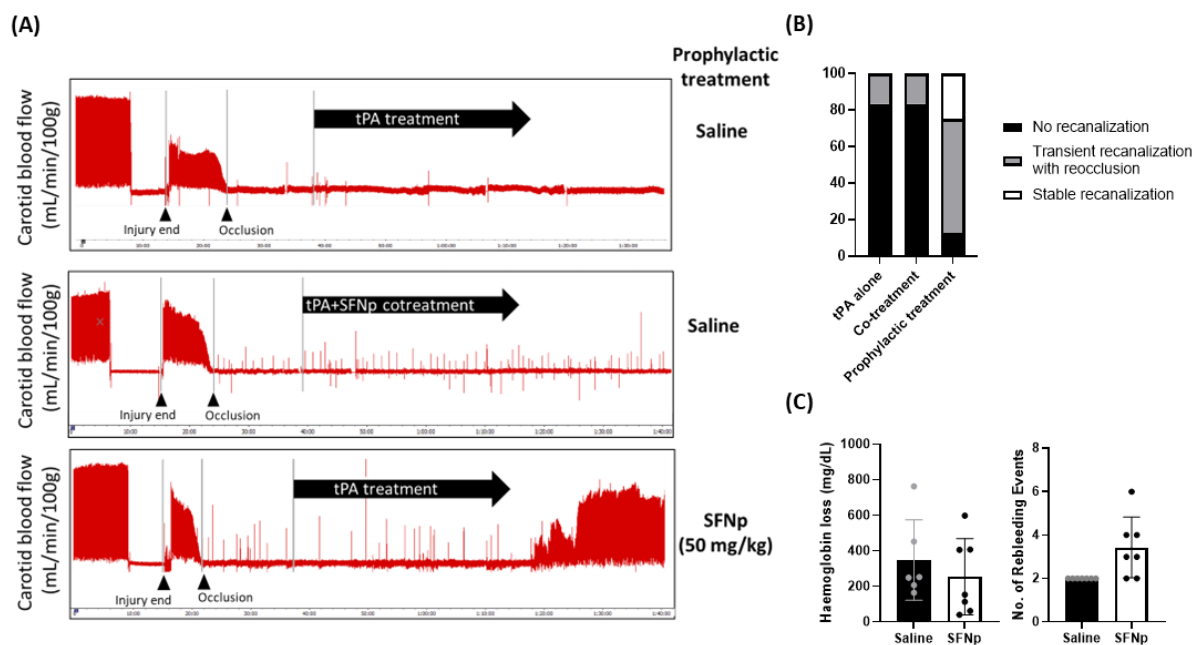


**Figure 6. SFNp improves recanalization outcomes prophylactically and does not increase bleeding. (A)** Real-time flow traces at baseline and following electrolytic injury: tPA treatment administered 15 minutes after stable occlusion (top panel), co-treatment of tPA and SFNp given 15 minutes after stable occlusion (middle panel), and prophylactic SFNp treatment applied 1 hour before injury followed by tPA administration 15 minutes post-injury (bottom panel). **(B)** Recanalization outcomes of treatment cohorts in **(A)** as described. **(C)** Tail bleeding outcomes demonstrate no significant difference in hemoglobin loss (left) when comparing a treatment with 50 mg/kg SFNp to an equal volume of saline treatment. The

number of rebleeding events (right) when mice were treated with 50 mg/kg SFNp or saline are shown.

**CONCLUSION:** The pursuit of selective intervention with platelet-mediated thrombus formation without disturbing hemostatic balance is a hot topic in cardiovascular research and an ongoing design challenge intimately associated with the intertwined signaling pathways underlying platelet activation. In this study, we combined a streamlined cell preparation method with antiplatelet phenotyping of electrophilic phytochemicals to uncover previously unknown agonist selectivity profiles. These profiles are associated with the impact of electrophilic protein modifications induced by these phytochemicals, thereby uncovering new insights into their mode of action. In particular, by combining ABPP, molecular simulation and mass-spectrometry analysis, we demonstrated that SFN serves as a novel chemotype for targeting PDIA6 in platelets, with mapping of the covalent modification sites revealing unparalleled levels of PDI isoform selectivity. Through interactome co-precipitation in conjunction with bioinformatic analysis, we elucidated the impact of SFN on PDIA6's substrate preference, which aligns with the observed *in vitro* and *in vivo* antiplatelet phenotypes. Importantly, SFN displayed important characteristics of prophylactic agents and was able to improve the clot-busting performance of rtPA in an *in vivo* electrolytic injury model of thrombosis. These results provide new insights into the studies of molecular pharmacology of naturally occurring isothiocyanates as novel antithrombotic leads, particularly in combination with approved therapies. Our findings also provide the impetus to investigate the molecular mechanisms underlying dietary antiplatelets with a view to discovering novel preventive and therapeutic mechanisms without significant bleeding risks.



## ASSOCIATED CONTENT

### Supporting Information.

## AUTHOR INFORMATION

### Corresponding Author

**Xuyu Liu** – School of Chemistry, Faculty of Science, The University of Sydney, Sydney, New South Wales 2006, Australia; The Heart Research Institute, The University of Sydney, Newtown, New South Wales 2042, Australia. Email: [xuyu.liu@sydney.edu.au](mailto:xuyu.liu@sydney.edu.au)

### First Author

**Ivy Guan** – School of Chemistry, Faculty of Science, The University of Sydney, Sydney, New South Wales 2006, Australia; The Heart Research Institute, The University of Sydney, Newtown, New South Wales 2042, Australia. Email: [ivy.guan@sydney.edu.au](mailto:ivy.guan@sydney.edu.au)

### Author Contributions

**I.A.G.** undertook initial platelet studies, proteomic research, chemical synthesis, and data analysis, and also participated in drafting the manuscript. **J.S.T.L.** executed all animal work, microslide perfusion studies, developed the corresponding figures, and assembled the references. **R.C.S.** completed the platelet aggregation studies and developed the corresponding figures. **Xiang L.** performed the integrated bioinformatic analysis and contributed to the development of bioinformatic methods and manuscript editing. **W.J.** carried out the computational studies and contributed to its method development and manuscript editing. **Y.J.** and **M.D.W.** were responsible for the PDIA6 protein expression. **L.H.** and **F.H.P.** offered guidance and insights into the development of PDIA6 assays and contributed to the manuscript editing. **D.P.T.** provided direction and insights into the development of the project-specific proteomic research method. **Xiaoming L.** contributed to the bioinformatic statistical analysis. **S.M.S.** and **S.P.J.** provided guidance and insights into developing murine models for testing dietary antiplatelets. **R.J.P.** provided guidance on the chemical synthesis strategy,

critically reviewed the manuscript and contributed to its writing. **Xuyu L.** conceptualized the project, critically reviewed the manuscript, contributed to writing and project administration, and secured funding. All authors were involved in the preparation of the supplementary information and the final proofreading of the manuscript.

### **Funding Sources**

The authors would like to acknowledge funding from the Sydney Cardiovascular Fellowship Scheme (to **Xuyu L.**), The University of Sydney Cardiovascular Initiative Catalyst Award (to **Xuyu L.**), The University of Sydney DDI-CVI Partnership Award (to **Xuyu L.**), the John A. Lamberton Scholarship (to **I.A.G.**), the Heart Research Institute Aotearoa Doctoral Student Award (to **I.A.G.** and **R.C.S.**), and the Australian Government RTP Scholarship (to **J.S.T.L.** and **Y.J.**).

### **Notes**

The authors declare that they have no competing interests.

### **ACKNOWLEDGMENTS**

Dr Ben Crossett (Associate Director of Sydney Mass Spectrometry at the University of Sydney) is acknowledged for his assistance in proteomic data analysis. Dr Nick Proschogo (Professional Officer – Mass Spectrometry at the School of Chemistry, The University of Sydney) is acknowledged for his assistance in producing HRMS data. Multiple figures were created with BioRender.com. The MD simulation was performed on the Rāpoi High-Performance Computing facility of Victoria University of Wellington.

## REFERENCES

1. Jackson SP. Arterial thrombosis—insidious, unpredictable and deadly. *Nature Medicine*. 2011;17(11):1423-36.
2. Pivkin IV, Richardson PD, Karniadakis G. Blood flow velocity effects and role of activation delay time on growth and form of platelet thrombi. *Proceedings of the National Academy of Sciences*. 2006;103(46):17164-9.
3. Stoll G, Nieswandt B. Thrombo-inflammation in acute ischaemic stroke — implications for treatment. *Nature Reviews Neurology*. 2019;15(8):473-81.
4. Koupenova M, Kehrel BE, Corkrey HA, Freedman JE. Thrombosis and platelets: an update. *European Heart Journal*. 2017;38(11):785-91.
5. Raskob GE, Angchaisuksiri P, Blanco AN, Buller H, Gallus A, Hunt BJ, et al. Thrombosis. *Arteriosclerosis, Thrombosis, and Vascular Biology*. 2014;34(11):2363-71.
6. Global Health Estimates: Life expectancy and leading causes of death and disability: World Health Organisation; 2023 [Available from: <https://www.who.int/data/gho/data/themes/mortality-and-global-health-estimates>].
7. Tyagi T, Jain K, Gu SX, Qiu M, Gu VW, Melchinger H, et al. A guide to molecular and functional investigations of platelets to bridge basic and clinical sciences. *Nature Cardiovascular Research*. 2022;1(3):223-37.
8. Serebruany VL, Malinin AI, Eisert RM, Sane DC. Risk of bleeding complications with antiplatelet agents: Meta-analysis of 338,191 patients enrolled in 50 randomized controlled trials. *American Journal of Hematology*. 2004;75(1):40-7.
9. Liu JST, Ding Y, Schoenwaelder S, Liu X. Improving treatment for acute ischemic stroke—Clot busting innovation in the pipeline. *Frontiers in Medical Technology*. 2022;4.
10. Derex L, Paris C, Nighoghossian N. Combining Intravenous Thrombolysis and Antithrombotic Agents in Stroke: An Update. *Journal of the American Heart Association*. 2018;7(2).

11. Napolitano F, Montuori N. Role of Plasminogen Activation System in Platelet Pathophysiology: Emerging Concepts for Translational Applications. *International Journal of Molecular Sciences*. 2022;23(11):6065.
12. Kellert L, Hametner C, Rohde S, Bendszus M, Hacke W, Ringleb P, et al. Endovascular Stroke Therapy. *Stroke*. 2013;44(5):1453-5.
13. Xie Q, Li H, Lu D, Yuan J, Ma R, Li J, et al. Neuroprotective Effect for Cerebral Ischemia by Natural Products: A Review. *Frontiers in Pharmacology*. 2021;12(607412).
14. Larsson SC. Dietary Approaches for Stroke Prevention. *Stroke*. 2017;48(10):2905-11.
15. Violi F, Pastori D, Pignatelli P, Carnevale R. Nutrition, Thrombosis, and Cardiovascular Disease. *Circulation Research*. 2020;126(10):1415-42.
16. Wang G, Ji Y, Li Z, Han X, Guo N, Song Q, et al. Nitro-oleic acid downregulates lipoprotein-associated phospholipase A2 expression via the p42/p44 MAPK and NFκB pathways. *Scientific Reports*. 2014;4(1).
17. Phang M, Lazarus S, Wood LG, Garg M. Diet and Thrombosis Risk: Nutrients for Prevention of Thrombotic Disease. *Seminars in Thrombosis and Hemostasis*. 2011;37(03):199-208.
18. Cassidy A, Rimm EB, O'Reilly ÉJ, Logroscino G, Kay C, Chiuve SE, et al. Dietary Flavonoids and Risk of Stroke in Women. *Stroke*. 2012;43(4):946-51.
19. Langston-Cox AG, Anderson D, Creek DJ, Palmer KR, Marshall SA, Wallace EM. Sulforaphane Bioavailability and Effects on Blood Pressure in Women with Pregnancy Hypertension. *Reproductive Sciences*. 2021;28(5):1489-97.
20. Arshad L, Jantan I, Bukhari SNA, Haque MA. Immunosuppressive Effects of Natural  $\alpha,\beta$ -Unsaturated Carbonyl-Based Compounds, and Their Analogs and Derivatives, on Immune Cells: A Review. *Frontiers in Pharmacology*. 2017;8.
21. Fernández-Rojas M, Rodríguez L, Trostchansky A, Fuentes E. Regulation of platelet function by natural bioactive compounds. *Food Bioscience*. 2022;48:101742.

22. Kamal RM, Ahmad FAR, Nurul SMS, Perimal EK, Ahmad H, Patrick R, et al. Beneficial Health Effects of Glucosinolates-Derived Isothiocyanates on Cardiovascular and Neurodegenerative Diseases. *Molecules*. 2022;27(3):624.
23. Stefanson AL, Bakovic M. Dietary Regulation of Keap1/Nrf2/ARE Pathway: Focus on Plant-Derived Compounds and Trace Minerals. *Nutrients*. 2014;6(9):3777-801.
24. Surguchov A, Bernal L, Surguchev AA. Phytochemicals as Regulators of Genes Involved in Synucleinopathies. *Biomolecules*. 2021;11(5):624.
25. Bhattacharjee S, Dashwood RH. Epigenetic Regulation of NRF2/KEAP1 by Phytochemicals. *Antioxidants*. 2020;9(9):865.
26. Burkhart JM, Gambaryan S, Watson SP, Jurk K, Walter U, Sickmann A, et al. What Can Proteomics Tell Us About Platelets? *Circulation Research*. 2014;114(7):1204-19.
27. Zimmerman GA, Weyrich AS. Signal-Dependent Protein Synthesis by Activated Platelets. *Arteriosclerosis, Thrombosis, and Vascular Biology*. 2008;28(3):s17-s24.
28. Tocmo R, Veenstra JP, Huang Y, Johnson JJ. Covalent Modification of Proteins by Plant-Derived Natural Products: Proteomic Approaches and Biological Impacts. *Proteomics*. 2021;21(3-4):1900386.
29. Liang H, Liu H, Kuang Y, Chen L, Ye M, Lai L. Discovery of Targeted Covalent Natural Products against PLK1 by Herb-Based Screening. *Journal of Chemical Information and Modeling*. 2020;60(9):4350-8.
30. Ishii T, Mori T, Tanaka T, Mizuno D, Yamaji R, Kumazawa S, et al. Covalent modification of proteins by green tea polyphenol (–)-epigallocatechin-3-gallate through autoxidation. *Free Radical Biology and Medicine*. 2008;45(10):1384-94.
31. Gaspar RS, da Silva SA, Stapleton J, Fontelles JLdL, Sousa HR, Chagas VT, et al. Myricetin, the Main Flavonoid in *Syzygium cumini* Leaf, Is a Novel Inhibitor of Platelet Thiol Isomerases PDI and ERp5. *Frontiers in Pharmacology*. 2020;10(1678).
32. Spradlin JN, Hu X, Ward CC, Brittain SM, Jones MD, Ou L, et al. Harnessing the anti-cancer natural product nimbolide for targeted protein degradation. *Nature Chemical Biology*. 2019;15(7):747-55.

33. Cui T, Wang Q, Tian X, Zhang K, Peng Y, Zheng J. Piperine Is a Mechanism-Based Inactivator of CYP3A. *Drug Metabolism and Disposition*. 2020;48(2):123-34.
34. Kim HG, Lee HS, Jeon JS, Choi YJ, Choi YJ, Yoo SY, et al. Quasi-Irreversible Inhibition of CYP2D6 by Berberine. *Pharmaceutics*. 2020;12(10):916.
35. Chang HC, Doerge DR, Hsieh C, Lin Y, Tsai F. The Covalent Binding of Genistein to the Non-prosthetic-heme-moiety of Bovine Lactoperoxidase Leads to Enzymatic Inactivation. *Biomedical and Environmental Sciences*. 2011;24(3):284-90.
36. Mons E, Roet S, Kim RQ, Mulder MPC. A Comprehensive Guide for Assessing Covalent Inhibition in Enzymatic Assays Illustrated with Kinetic Simulations. *Current Protocols*. 2022;2(6):e419.
37. Copeland RA, Basavapathruni A, Moyer M, Scott MP. Impact of enzyme concentration and residence time on apparent activity recovery in jump dilution analysis. *Analytical Biochemistry*. 2011;416(2):206-10.
38. Kao CC, Kung PH, Tai CJ, Tsai MC, Cheng YB, Wu CC. Juglone prevents human platelet aggregation through inhibiting Akt and protein disulfide isomerase. *Phytomedicine*. 2021;82:153449.
39. Santhakumar AB, Bulmer AC, Singh I. A review of the mechanisms and effectiveness of dietary polyphenols in reducing oxidative stress and thrombotic risk. *Journal of Human Nutrition and Dietetics*. 2014;27(1):1-21.
40. Ku S, Lee I, Kim J, Bae J. Antithrombotic activities of pellitorine in vitro and in vivo. *Fitoterapia*. 2013;91:1-8.
41. Wu Y, Deng C, Wang Y, Ming Z, Mei H, Hu Y. The inhibitory effect of isoliquiritigenin on human platelets in vitro. *Annals of Translational Medicine*. 2023;11(6):250.
42. Jackson SP, Schoenwaelder SM. Antiplatelet therapy: in search of the 'magic bullet'. *Nature Reviews Drug Discovery*. 2003;2(10):775-89.
43. Negrier C, Shima M, Hoffman M. The central role of thrombin in bleeding disorders. *Blood Reviews*. 2019;38:100582.

44. Soslau G, Class R, Morgan DA, Foster C, Lord ST, Marchese P, et al. Unique Pathway of Thrombin-induced Platelet Aggregation Mediated by Glycoprotein Ib. *Journal of Biological Chemistry*. 2001;276(24):21173-83.
45. Cauwenberghs N, Meiring M, Vauterin S, Van Wyk V, Lamprecht S, Roodt JP, et al. Antithrombotic Effect of Platelet Glycoprotein Ib–Blocking Monoclonal Antibody Fab Fragments in Nonhuman Primates. *Arteriosclerosis, Thrombosis, and Vascular Biology*. 2000;20(5):1347-53.
46. Ramakrishnan V, Deguzman F, Bao M, Hall SW, Leung LL, Phillips DR. A thrombin receptor function for platelet glycoprotein Ib–IX unmasked by cleavage of glycoprotein V. *Proceedings of the National Academy of Sciences*. 2001;98(4):1823-8.
47. Kulkarni S, Nesbitt WS, Dopheide SM, Hughan SC, Harper IS, Jackson SP. Techniques to Examine Platelet Adhesive Interactions Under Flow. *Platelets and Megakaryocytes*. 272: Humana Press; 2004. p. 165-86.
48. Ahn YH, Hwang Y, Liu H, Wang XJ, Zhang Y, Stephenson KK, et al. Electrophilic Tuning of the Chemoprotective Natural Product Sulforaphane. *Proceedings of the National Academy of Sciences*. 2010;107(21):9590-5.
49. Clulow JA, Storck EM, Lanyon-Hogg T, Kalesh KA, Jones LH, Tate EW. Competition-based, quantitative chemical proteomics in breast cancer cells identifies new target profiles for sulforaphane. *Chemical Communications*. 2017;53(37):5182-5.
50. Chuang WY, Kung PH, Kuo CY, Wu CC. Sulforaphane prevents human platelet aggregation through inhibiting the phosphatidylinositol 3-kinase/Akt pathway. *Thrombosis and Haemostasis*. 2013;109(06):1120-30.
51. Gillespie S, Holloway PM, Becker F, Rauzi F, Vital SA, Taylor KA, et al. The isothiocyanate sulforaphane modulates platelet function and protects against cerebral thrombotic dysfunction. *British Journal of Pharmacology*. 2018;175(16):3333-46.
52. Roberts AM, Ward CC, Nomura DK. Activity-based protein profiling for mapping and pharmacologically interrogating proteome-wide ligandable hotspots. *Current Opinion in Biotechnology*. 2017;43:25-33.

53. Chan WC, Sharifzadeh S, Buhrlage SJ, Marto JA. Chemoproteomic methods for covalent drug discovery. *Chemical Society Reviews*. 2021;50(15):8361-81.
54. Boike L, Henning NJ, Nomura DK. Advances in covalent drug discovery. *Nature Reviews Drug Discovery*. 2022;21(12):881-98.
55. Backus KM, Correia BE, Lum KM, Forli S, Horning BD, González-Páez GE, et al. Proteome-wide Covalent Ligand Discovery in Native Biological Systems. *Nature*. 2016;534(7608):570-4.
56. Bennis HJ, Wincott CJ, Tate EW, Child MA. Activity- and reactivity-based proteomics: Recent technological advances and applications in drug discovery. *Current Opinion in Chemical Biology*. 2021;60:20-9.
57. Liu X, Long MJC, Hopkins BD, Luo C, Wang L, Aye Y. Precision Targeting of pten-Null Triple-Negative Breast Tumors Guided by Electrophilic Metabolite Sensing. *ACS Central Science*. 2020;6(6):892-902.
58. Liu X, Long MJC, Aye Y. Proteomics and Beyond: Cell Decision-Making Shaped by Reactive Electrophiles. *Trends in Biochemical Sciences*. 2019;44(1):75-89.
59. Zhao Y, Miranda Herrera PA, Chang D, Hamelin R, Long MJC, Aye Y. Function-guided proximity mapping unveils electrophilic-metabolite sensing by proteins not present in their canonical locales. *Proceedings of the National Academy of Sciences*. 2022;119(5):e2120687119.
60. Zhu H, Tamura T, Hamachi I. Chemical proteomics for subcellular proteome analysis. *Current Opinion in Chemical Biology*. 2019;48:1-7.
61. Yasueda Y, Tamura T, Fujisawa A, Kuwata K, Tsukiji S, Kiyonaka S, et al. A Set of Organelle-Localizable Reactive Molecules for Mitochondrial Chemical Proteomics in Living Cells and Brain Tissues. *Journal of the American Chemical Society*. 2016;138(24):7592-602.
62. Matthews ML, He L, Horning BD, Olson EJ, Correia BE, Yates JR, et al. Chemoproteomic profiling and discovery of protein electrophiles in human cells. *Nature Chemistry*. 2017;9(3):234-43.



63. Wiedner SD, Anderson LN, Sadler NC, Chrisler WB, Kodali VK, Smith RD, et al. Organelle-Specific Activity-Based Protein Profiling in Living Cells. *Angewandte Chemie International Edition*. 2014;53(11):2919-22.
64. Grainger DJ, Wakefield L, Bethell HW, Farndale RW, Metcalfe JC. Release and activation of platelet latent TGF- $\beta$  in blood clots during dissolution with plasmin. *Nature Medicine*. 1995;1(9):932-7.
65. Mitchell WB, Li JH, French DL, Collier BS.  $\alpha$ IIb $\beta$ 3 biogenesis is controlled by engagement of  $\alpha$ IIb in the calnexin cycle via the N15-linked glycan. *Blood*. 2006;107(7):2713-9.
66. Lay AJ, Dupuy A, Hagimola L, Tieng J, Larance M, Zhang Y, et al. Endoplasmic reticulum protein 5 attenuates platelet endoplasmic reticulum stress and secretion in a mouse model. *Blood Advances*. 2023;7(9):1650-65.
67. Passam FH, Chiu J, Ju L, Pijning A, Jahan Z, Mor-Cohen R, et al. Mechano-redox control of integrin de-adhesion. *eLife*. 2018;7:e34843.
68. Passam FH, Lin L, Gopal S, Stopa JD, Bellido-Martin L, Huang M, et al. Both platelet- and endothelial cell-derived ERp5 support thrombus formation in a laser-induced mouse model of thrombosis. *Blood*. 2015;125(14):2276-85.
69. Chiu J, Passam F, Butera D, Hogg PJ. Protein Disulfide Isomerase in Thrombosis. *Seminars in Thrombosis and Hemostasis*. 2015;41(07):765-73.
70. Chiu J, Hogg PJ. Allosteric disulfides: Sophisticated molecular structures enabling flexible protein regulation. *Journal of Biological Chemistry*. 2019;294(8):2949-5908.
71. Appenzeller-Herzog C, Ellgaard L. The human PDI family: Versatility packed into a single fold. *Biochimica et Biophysica Acta (BBA) - Molecular Cell Research*. 2008;1783(4):535-48.
72. Holmgren A. Thioredoxin catalyzes the reduction of insulin disulfides by dithiothreitol and dihydrolipoamide. *Journal of Biological Chemistry*. 1979;254(19):9627-32.

73. Chinnaraj M, Flaumenhaft R, Pozzi N. Reduction of protein disulfide isomerase results in open conformations and stimulates dynamic exchange between structural ensembles. *Journal of Biological Chemistry*. 2022;298(8):102217.
74. Jumper J, Evans R, Pritzel A, Green T, Figurnov M, Ronneberger O, et al. Highly accurate protein structure prediction with AlphaFold. *Nature*. 2021;596(7873):583-9.
75. Halgren TA. Identifying and Characterizing Binding Sites and Assessing Druggability. *Journal of Chemical Information and Modeling*. 2009;49(2):377-89.
76. Halgren T. New Method for Fast and Accurate Binding-site Identification and Analysis. *Chemical Biology & Drug Design*. 2007;69(2):146-8.
77. Friesner RA, Murphy RB, Repasky MP, Frye LL, Greenwood JR, Halgren TA, et al. Extra Precision Glide: Docking and Scoring Incorporating a Model of Hydrophobic Enclosure for Protein–Ligand Complexes. *Journal of Medicinal Chemistry*. 2006;49(21):6177-96.
78. Halgren TA, Murphy RB, Friesner RA, Beard HS, Frye LL, Pollard WT, et al. Glide: A New Approach for Rapid, Accurate Docking and Scoring. 2. Enrichment Factors in Database Screening. *Journal of Medicinal Chemistry*. 2004;47(7):1750-9.
79. Friesner RA, Banks JL, Murphy RB, Halgren TA, Klicic JJ, Mainz DT, et al. Glide: A New Approach for Rapid, Accurate Docking and Scoring. 1. Method and Assessment of Docking Accuracy. *Journal of Medicinal Chemistry*. 2004;47(7):1739-49.
80. Farid R, Day T, Friesner RA, Pearlstein RA. New insights about HERG blockade obtained from protein modeling, potential energy mapping, and docking studies. *Bioorganic & Medicinal Chemistry*. 2006;14(9):3160-73.
81. Sherman W, Day T, Jacobson MP, Friesner RA, Farid R. Novel Procedure for Modeling Ligand/Receptor Induced Fit Effects. *Journal of Medicinal Chemistry*. 2006;49(2):534-53.
82. Sherman W, Beard HS, Farid R. Use of an Induced Fit Receptor Structure in Virtual Screening. *Chemical Biology & Drug Design*. 2006;67(1):83-4.
83. Cosemans JMEM, Munnix ICA, Wetzker R, Heller R, Jackson SP, Heemskerk JWM. Continuous signaling via PI3K isoforms  $\beta$  and  $\gamma$  is required for platelet ADP receptor function in dynamic thrombus stabilization. *Blood*. 2006;108(9):3045-52.

84. Jackson SP, Schoenwaelder SM, Goncalves I, Nesbitt WS, Yap CL, Wright CE, et al. PI 3-kinase p110 $\beta$ : a new target for antithrombotic therapy. *Nature Medicine*. 2005;11(5):507-14.
85. Gilio K, Munnix ICA, Mangin P, Cosemans JMEM, Feijge MAH, Van Der Meijden PEJ, et al. Non-redundant Roles of Phosphoinositide 3-Kinase Isoforms  $\alpha$  and  $\beta$  in Glycoprotein VI-induced Platelet Signaling and Thrombus Formation. *Journal of Biological Chemistry*. 2009;284(49):33750-62.
86. Comer SP. Turning Platelets Off and On: Role of RhoGAPs and RhoGEFs in Platelet Activity. *Frontiers in Cardiovascular Medicine*. 2022;8:820945.
87. Ono A, Westein E, Hsiao S, Nesbitt WS, Hamilton JR, Schoenwaelder SM, et al. Identification of a fibrin-independent platelet contractile mechanism regulating primary hemostasis and thrombus growth. *Blood*. 2008;112(1):90-9.
88. Moretti AIS, Pavanelli JC, Nolasco P, Leisegang MS, Tanaka LY, Fernandes CG, et al. Conserved Gene Microsynteny Unveils Functional Interaction Between Protein Disulfide Isomerase and Rho Guanine-Dissociation Inhibitor Families. *Scientific Reports*. 2017;7(1):17262.
89. Pescatore LA, Bonatto D, Forti FL, Sadok A, Kovacic H, Laurindo FRM. Protein Disulfide Isomerase Is Required for Platelet-derived Growth Factor-induced Vascular Smooth Muscle Cell Migration, Nox1 NADPH Oxidase Expression, and RhoGTPase Activation. *Journal of Biological Chemistry*. 2012;287(35):29290-300.
90. Varga-Szabo D, Braun A, Nieswandt B. STIM and Orai in platelet function. *Cell Calcium*. 2011;50(3):270-8.
91. Maclean JAA, Tomkins AJ, Sturgeon SA, Hofma BR, Alwis I, Samson AL, et al. Development of a carotid artery thrombolysis stroke model in mice. *Blood Advances*. 2022;6(18):5449-62.
92. Schoenwaelder SM, Jarman KE, Gardiner EE, Hua M, Qiao J, White MJ, et al. Bcl-xL-inhibitory BH3 mimetics can induce a transient thrombocytopenia that undermines the hemostatic function of platelets. *Blood*. 2011;118(6):1663-74.

